

Introduction

Gamma band oscillations recorded in vivo appear usually as discrete events of synchrony called gamma bursts. The overall process is a random signal closer to a filtered noise than a coherent oscillation [1]. Despite its randomness, it has been showed that such bursty gamma oscillations are good candidates for inter-areal brain communication [2]. The communication function implied synchronization between connected bursty gamma oscillatory brain areas. Here we investigated phase synchronization and information transfer between identical connected networks of PING type. More specifically we derived envelope-phase equations of the two identical networks. The phases dynamics derived analytically allow to show the parameters responsible for synchronization. We found that noise and propagation delay between the networks induce Out-of-phase locking (bi-stability in the correlation function between the phase dynamics of the coupled networks), whereas zero propagation delay always leads to In-phase locking. We computed delayed mutual information between phase dynamics of the two connected networks and showed that the type of phase locking (In-phase or Out-of-phase) was in agreement with the structure of mutual information, clearly the presence of propagation delay was able to allow for two distinct routes of communication similar to what has been showed in other study [2].

Synchronization in gamma bursty networks

Networks of excitatory (E_1 : blue) and (E_2 : red) neurons with two-state dynamics (active and quiescent) show oscillations in the gamma band (30-90 Hz) due to stochastically recurring epochs of high synchrony, i.e. Gamma bursts.

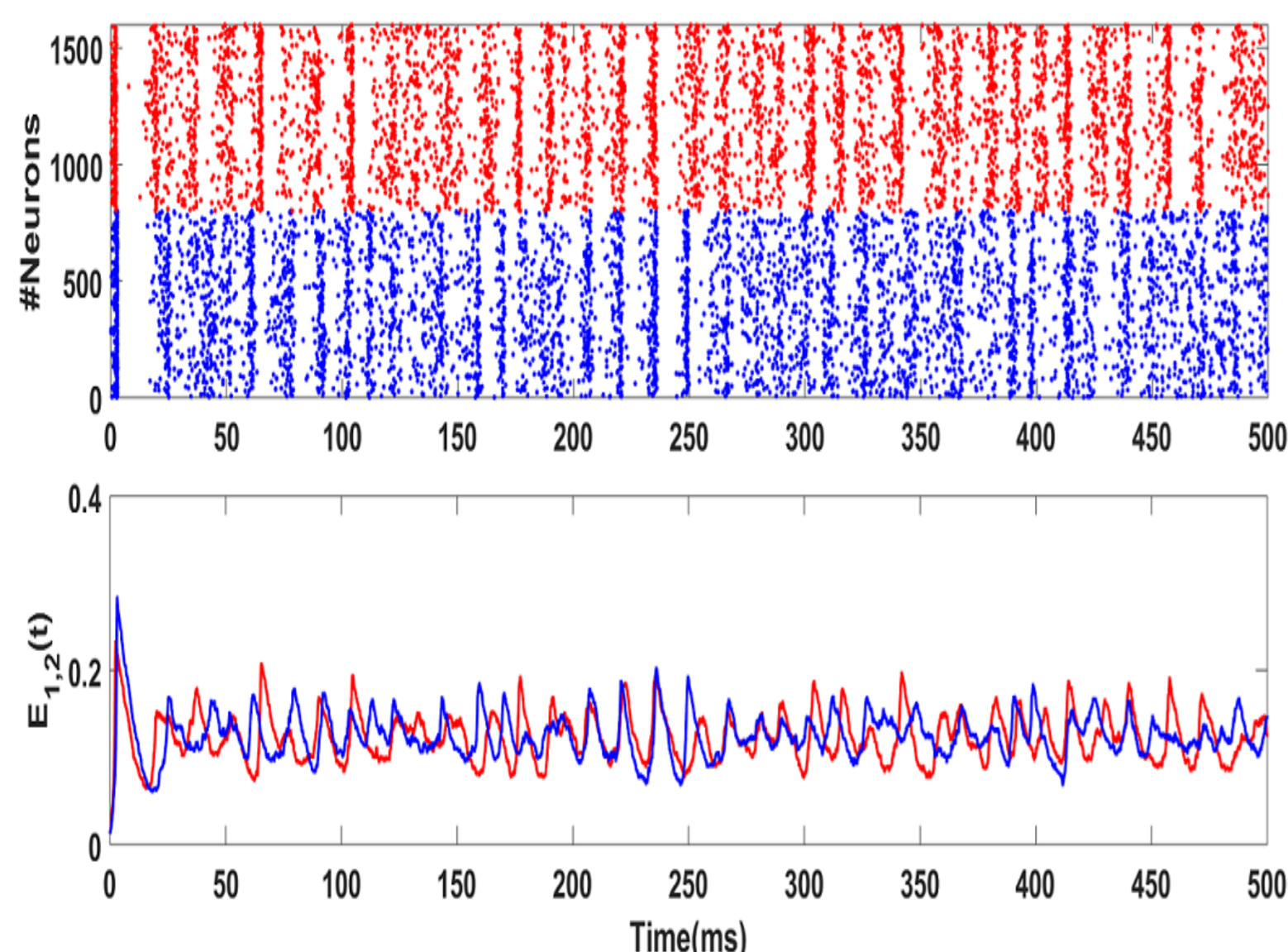


Figure 1: Top: Rasters, Bottom: Activities. Coupled networks show epochs of synchronized activities during gamma bursts. Only excitatory neurons are shown.

From Poisson process analysis, E_i and I_i ($i=1,2$) activities are given by nonlinear stochastic equations (stochastic Wilson-Cowan equations) [3]:

$$\frac{dE_i(t)}{dt} = -\alpha_E E_i(t) + (1 - E_i(t))\beta_E f(s_{E_i}(t)) + \sqrt{\frac{(1 - E_i(t))\beta_E f(s_{E_i}(t)) + \alpha_E E_i(t)}{N_E}} \xi_{E_i}(t)$$

$$\frac{dI_i(t)}{dt} = -\alpha_I I_i(t) + (1 - I_i(t))\beta_I f(s_{I_i}(t)) + \sqrt{\frac{(1 - I_i(t))\beta_I f(s_{I_i}(t)) + \alpha_I I_i(t)}{N_I}} \xi_{I_i}(t)$$

$$s_{E_i}(t) = W_{EE}E_i(t) - W_{EI}I_i(t) + h_E^i + L_{EE}^{ij}E_j(t - \tau)$$

$$s_{I_i}(t) = W_{IE}E_i(t) - W_{II}I_i(t) + h_I^i + L_{IE}^{ij}E_j(t - \tau)$$

The deterministic analogue in the thermodynamic limit admit a fixed point with damped oscillations, therefore the system above admits a quasi-cycle attractor.

Envelope and phase equations for E_i and I_i

We are interested in the fluctuations from the baseline activities (LNA)[3]: $V_E^i(t) = \sqrt{N_E}(E_i(t) - E_0)$; $V_I^i(t) = \sqrt{N_I}(I_i(t) - I_0)$ Where E_0 and I_0 are the deterministic fixed point activities.

Stochastic Averaging Method [3] leads to an envelope-phase representation in terms of key parameters ($D, \omega, \Omega, C_{EE}, C_{IE}, \lambda, \alpha, \delta, \tau$)

$$\begin{aligned} dZ_1(t) &= \left(-\lambda Z_1(t) + M_1(\phi_1(t) - \phi_2(t - \tau))Z_2(t - \tau) + \frac{D}{2Z_1(t)} \right) dt + \sqrt{D}dW_{Z_1}(t) \\ d\phi_1(t) &= \left(\Omega + M_1(\phi_1(t) - \phi_2(t - \tau))\frac{Z_2(t - \tau)}{Z_1(t)} \right) dt + \frac{\sqrt{D}}{Z_1(t)}dW_{\phi_1}(t) \\ dZ_2(t) &= \left(-\lambda Z_2(t) + M_2(\phi_2(t) - \phi_1(t - \tau))Z_1(t - \tau) + \frac{D}{2Z_2(t)} \right) dt + \sqrt{D}dW_{Z_2}(t) \\ d\phi_2(t) &= \left(\Omega + M_2(\phi_2(t) - \phi_1(t - \tau))\frac{Z_1(t - \tau)}{Z_2(t)} \right) dt + \frac{\sqrt{D}}{Z_2(t)}dW_{\phi_2}(t) \end{aligned}$$

$$\begin{aligned} M_1(x) &= \frac{1}{\sin(\delta)} \left[C_{EE}\sin(x + \omega\tau + \delta) - C_{IE}\sin(x + \omega\tau - \delta) \right] \\ M_2(x) &= \frac{1}{\sin(\delta)} \left[C_{EE}\cos(x + \omega\tau + \delta) - C_{IE}\cos(x + \omega\tau - \delta) \right] \end{aligned}$$

Then

$$\begin{aligned} V_E^1(t) &= Z_1(t) \cos(\omega t + \phi_1(t)); & V_I^1(t) &= \alpha Z_1(t) \cos(\omega t + \phi_1(t) + \delta) \\ V_E^2(t) &= Z_2(t) \cos(\omega t + \phi_2(t)); & V_I^2(t) &= \alpha Z_2(t) \cos(\omega t + \phi_2(t) + \delta) \end{aligned}$$

• Gamma Envelope-phase dynamics for the coupled networks obtained from the LNA and SAM show epochs of phase-locking.

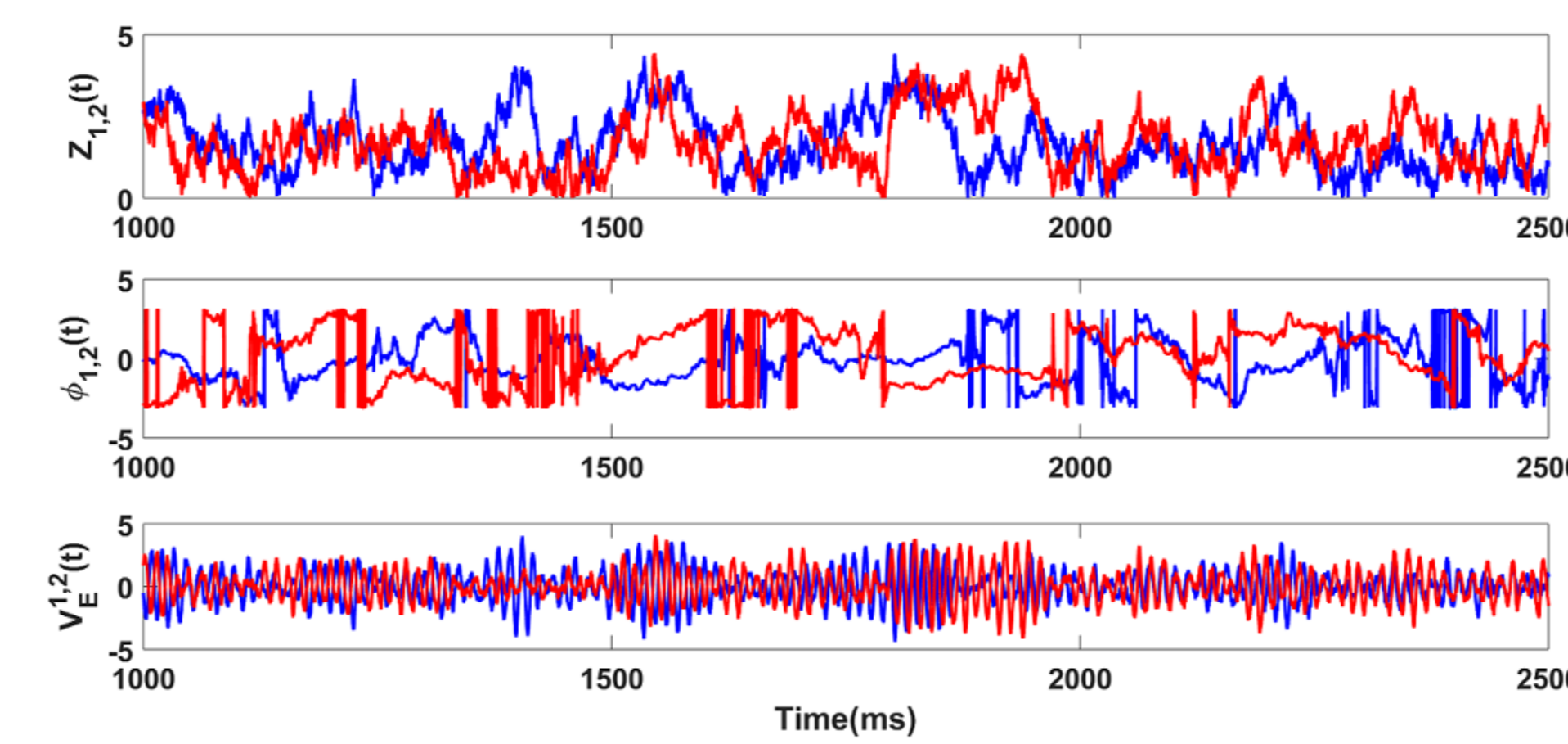


Figure 2: Envelopes, phases and LFPs time series for the E_1 (blue) and E_2 (red) populations. (Top) Envelopes time-series. (Middle) Phases time series. (Bottom) LFPs time series corresponding to the envelopes (top) and phases (middle) time series

Phase synchronization: inter-areal delay induces Out-of-phase locking

• Phase difference dynamics without delay ($\tau = 0ms$)

$$\begin{aligned} d\psi(t) &= - \left[C_{EE} + C_{IE} \right] \sin[\psi(t)] dt + \frac{\sqrt{D}}{Z_1(t)} dW_1(t) \\ f(\psi) &= - \left[C_{EE} + C_{IE} \right] \sin[\psi(t)]; & \psi(t) &= \phi_1(t) - \phi_2(t) \end{aligned}$$

The only deterministic stable solutions are ($\psi = 2k\pi, k = 0, 1, 2, \dots$): **In-phase locking only.**

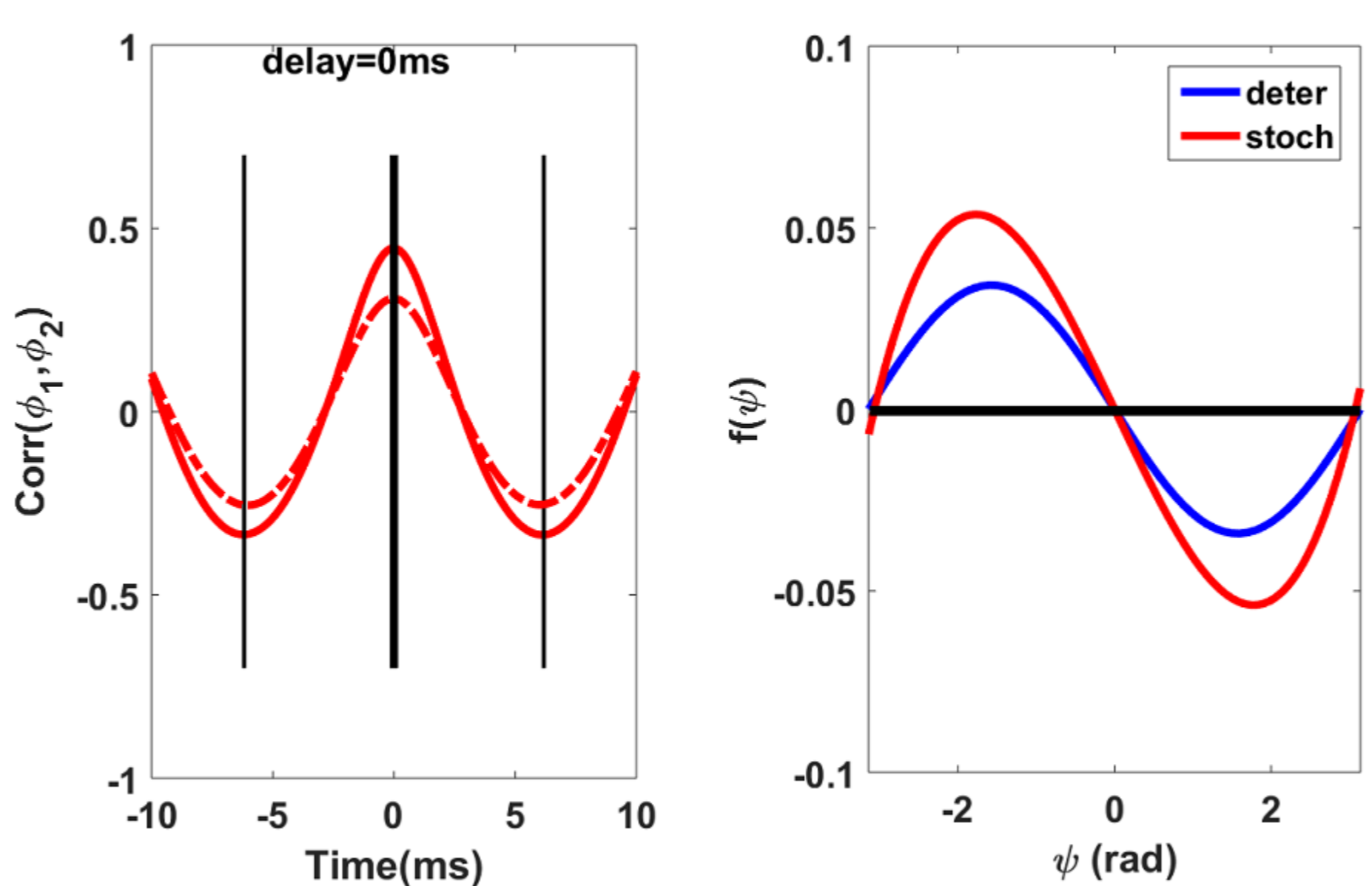


Figure 3: The coupled networks with zero propagation delay always exhibit In-phase locking. Left: Correlation function between the phase dynamics. vertical black bars correspond to $t = -T/2, 0, T/2$ where T is the period of the oscillation. The solid and dashed red lines represent respectively the cases where the phases are obtained via the Hilbert transform performed on former nonlinear dynamics and from the SAM. Right: Stability analysis of the phase difference dynamics. The phase difference dynamics admits a single stable fixed point at zero observed on both stochastic and deterministic functions. The deterministic function is obtained analytically after some approximations. For the stochastic function, we computed at each time step a stochastic function $F(x) = M_1(x)\frac{Z_2(t-\tau)}{Z_1(t)} - M_2(x)\frac{Z_1(t-\tau)}{Z_2(t)}$, we therefore fitted $F(x)$ with a polynomial function to obtain $f(x)$.

• Phase difference dynamics with delay ($\tau \neq 0ms$)

$$\begin{aligned} d\psi(t) &= -M_1 \left[\frac{\theta(t) - \theta(t - \tau)}{2} \right] \sin \left[\frac{\psi(t) + \psi(t - \tau)}{2} \right] dt + \frac{\sqrt{D}}{Z_1(t)} dW_1(t) \\ d\theta(t) &= M_2 \left[\frac{\theta(t) - \theta(t - \tau)}{2} \right] \cos \left[\frac{\psi(t) + \psi(t - \tau)}{2} \right] dt + \frac{\sqrt{D}}{Z_2(t)} dW_2(t) \\ f(\psi) &= \frac{1}{\sin(\delta)} \left[C_{IE}\sin(\omega\tau - \delta) - C_{EE}\sin(\omega\tau + \delta) \right] \sin(\psi); & \theta(t) &= \phi_1(t) + \phi_2(t) \end{aligned}$$

The only deterministic stable solutions depending on the values of $\omega, \tau, C_{IE}, C_{EE}$ are ($\psi = k\pi, k = 0, 1, 2, 3, \dots$): **In and Anti-phase locking only.**

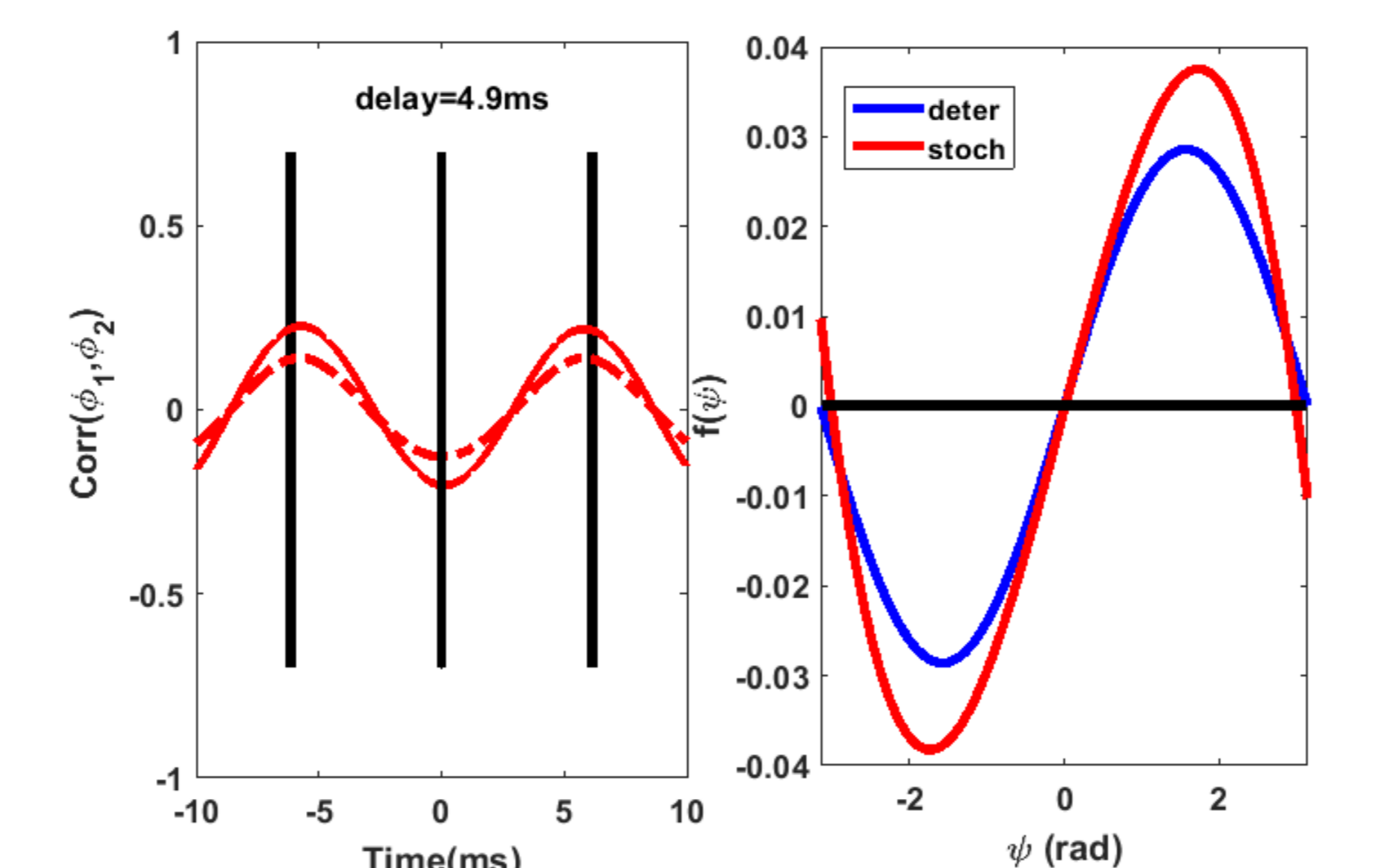


Figure 4: Propagation delay and noise cooperate to induce Out-of-phase locking different to Anti-phase locking. Left: We observe two symmetric peaks in the correlation function, the positions of the peaks are different to $-T/2$ and $T/2$ and suggest an Out-of-phase locking between the two populations. Right: The stability functions show an unstable fixed point at zero for both the stochastic and deterministic functions, however the positions of the two stable fixed points are $\psi^* = -\pi, \pi$ for the deterministic case and $\psi^* = -\beta, \beta$ with $|\beta| < \pi$ for the stochastic case.

• Bifurcation diagram: Out-of-phase locking

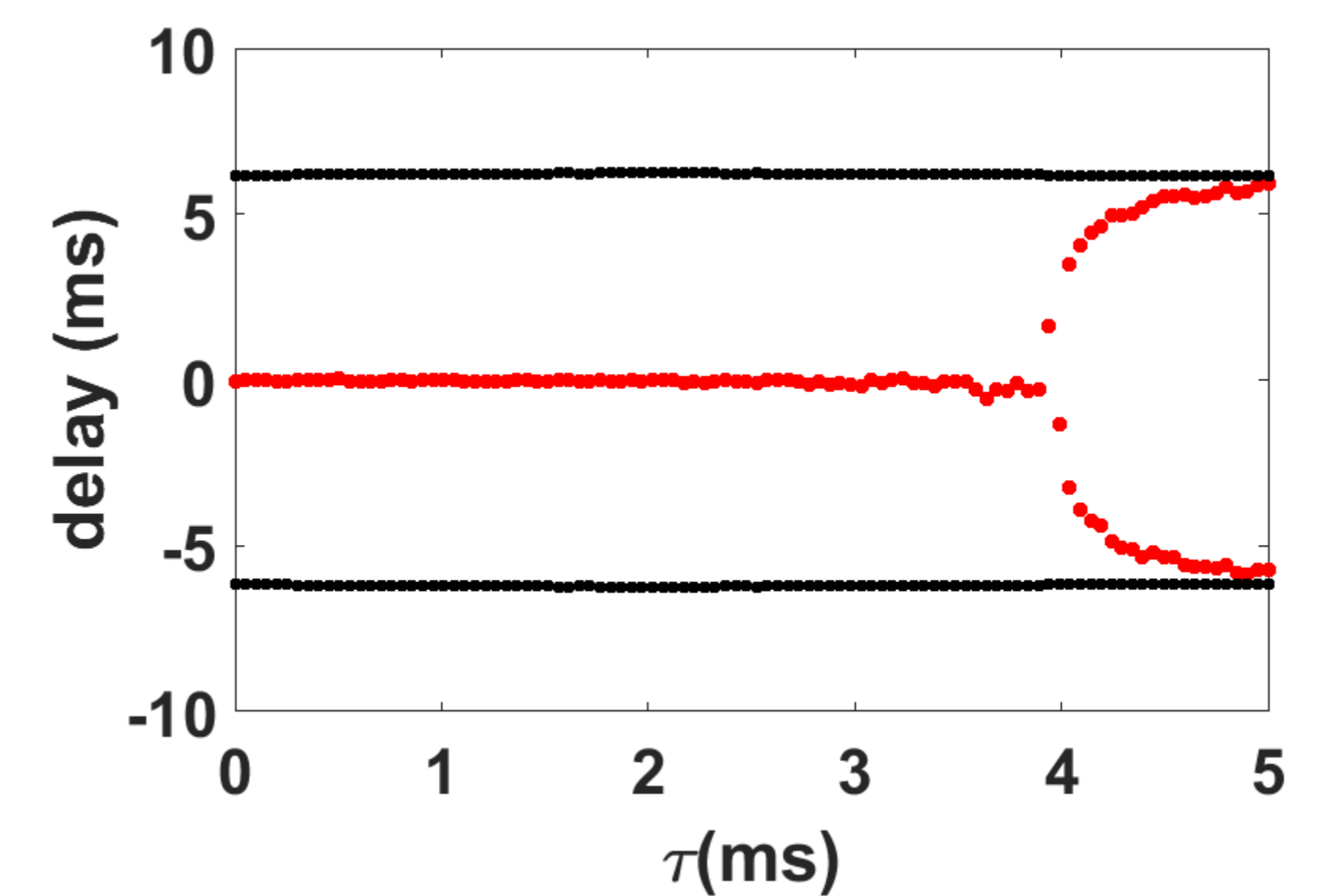


Figure 5: Bifurcation diagram showing the positions of the peaks of the correlation function as the propagation delay τ varies. We observe a clear bifurcation from an In-phase locking to an Out-of-phase locking (bistability in the correlation function) at a critical value of the inter-areal propagation delay. We have fixed the noise intensities at weak values ($N_E = 800000, N_I = 200000$). We recall that the deterministic case always leads to In-phase or Anti-phase locking (it can be seen through the function $f(x)$).

Information transfer through delayed mutual information

• We quantify information transfer through delayed Mutual information analysis.

$$MI(\tau)_{xy} = \sum P(y(t), x(t - \tau)) \log_2 \left(\frac{P(y(t), x(t - \tau))}{P(y(t))P(x(t - \tau))} \right)$$

• $\tau = 0ms$: No directionality for Information transfer

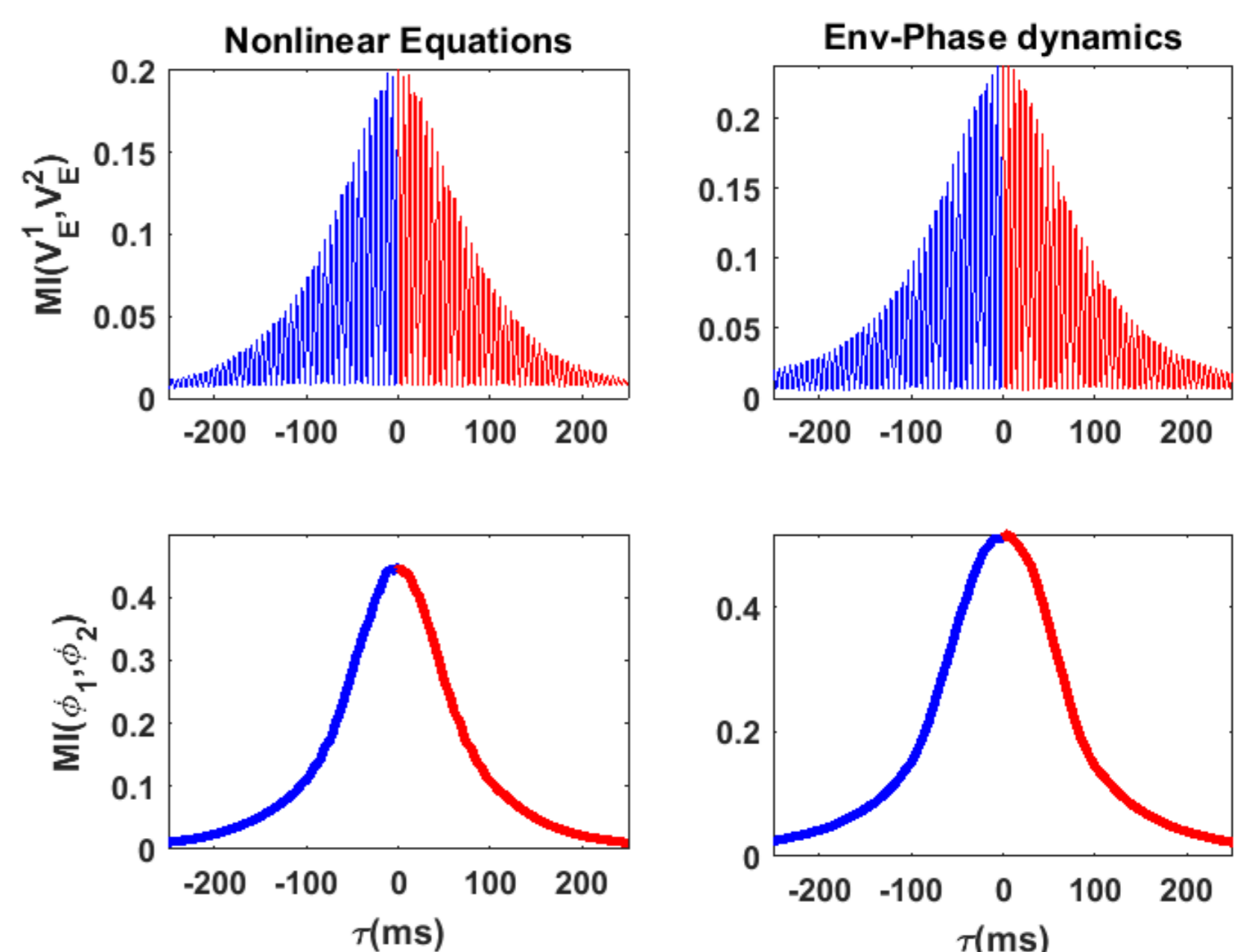


Figure 6: Delayed Mutual Information for coupled networks with no inter-areal propagation delay. The phase delayed Mutual information shows a single peak at $\tau = 0ms$. This suggests that there is not preferred direction for information flow. The information is transferred similarly from one network to the other and such transfer is maximal at $\tau = 0ms$ (In-phase locking).

• $\tau \neq 0ms$: Directionality for Information transfer

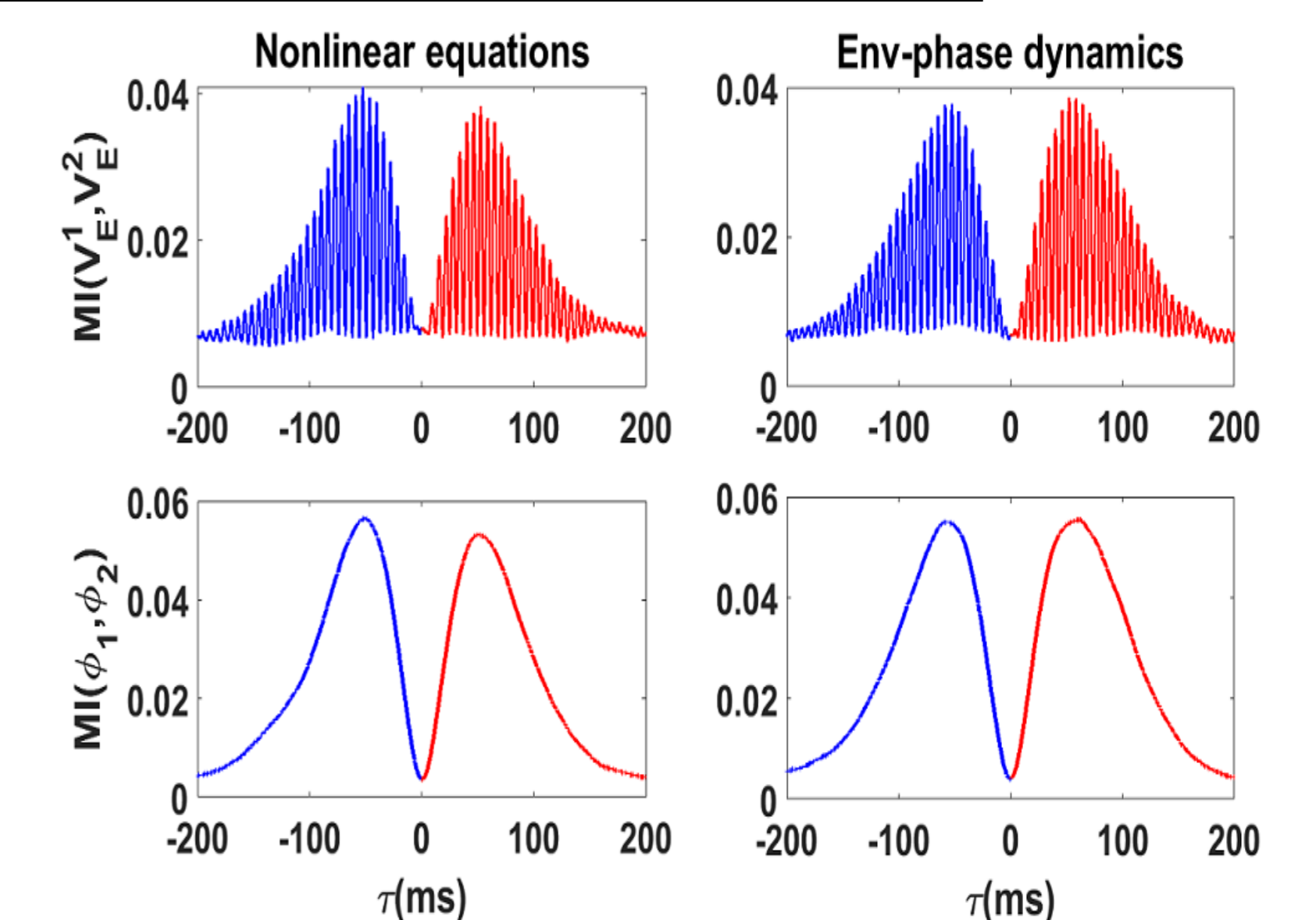


Figure 7: Delayed Mutual Information with inter-areal propagation delay shows a directionality and therefore the possibility for a flexible inter-areal communication. The phase delayed mutual information curves show two symmetric peaks positions different from zero. The two peaks correspond respectively to the situations where one of the networks is the leader while the other is the laggard and vice-versa. This suggests two routes for information transfer. The exact value of the delay conduction is set to $\tau = 4.1ms$.

Conclusion

We have derived the envelope-phase dynamics of a coupled bursty oscillatory networks in the gamma band. Our decomposition allows to relate phase synchronization on gamma bursts. In fact, phase synchronization is a transient process which happens more efficiently during bursts of the processes. In addition we have showed that inter-areal propagation delay and noise cooperate to induce out of phase locking which is crucial for bidirectional communication. Our study suggests that bursty oscillations which are ubiquitously observed in vivo are good candidate for flexible brain communication. Future studies will have the ambition to extend our study to more than two networks with heterogeneities.

Acknowledgments

This work was supported by NSERC Canada.

References: [1] D. Xing et al, *J. Neurosci*, **20**, 13873-13873a (2012).

[2] A. Palmigiano et al, *Nat. Neurosci*, **20**, 1014-1022 (2017).

[3] A. Powanwe et al, *Submitted*